

# Mixing times of organic molecules within secondary organic aerosol particles: a global planetary boundary layer perspective

Adrian M. Maclean<sup>1</sup>, Christopher L. Butenhoff<sup>2</sup>, James W. Grayson<sup>1</sup>, Kelley Barsanti<sup>3</sup>, Jose L. Jimenez<sup>4\*</sup>, Allan K. Bertram<sup>1\*</sup>

<sup>1</sup>Department of Chemistry, University of British Columbia, Vancouver, BC, V6T 1Z1, Canada

<sup>2</sup>Dept. of Physics, Portland State University, Portland, Oregon

<sup>3</sup>Department of Chemical and Environmental Engineering and Center for Environmental Research and Technology, University of California, Riverside

<sup>4</sup>Cooperative Institute for Research in the Environmental Sciences and Department of Chemistry and Biochemistry, University of Colorado, Boulder, CO, USA

\*To whom correspondence should be addressed. Allan K. Bertram (email): [bertram@chem.ubc.ca](mailto:bertram@chem.ubc.ca) and Jose L. Jimenez (email): [jose.jimenez@colorado.edu](mailto:jose.jimenez@colorado.edu)

## Supporting Information

### S1. Derivation of Equation 1 from the main text.

The WLF equation provides a relationship between viscosity and temperature:

$$\log\left(\frac{\eta}{\eta_g}\right) = \frac{-C_1(T-T_g)}{C_2+(T-T_g)} \quad (\text{S1})$$

where  $C_1$  and  $C_2$  are constants,  $T$  is the temperature,  $T_g$  is the glass transition temperature,  $\eta$  is the viscosity and  $\eta_g$  is the viscosity at the glass transition ( $10^{12}$  Pa s). The Gordon-Taylor equation provides a relationship between the glass transition temperature of a mixture and the weight fractions of its components:

$$T_{g,mix} = \frac{w_1 T_{g1} + w_2 T_{g2} k_{GT}}{w_1 + w_2 k_{GT}} \quad (\text{S2})$$

where  $w_1$  and  $w_2$  are the weight fractions of the solute and water,  $T_{g1}$  and  $T_{g2}$  are the glass transition temperatures of the solute and water, and  $k_{GT}$  is a fitting parameter that describes the interaction between the two species. Equations (S1) and (S2) can be combined to give Eq. (1) in the main text.

Equation (S1) (and hence Eq. (1)) is valid only at or above the glass transition temperature. As a result, we have not used Eq. (1) to predict viscosities  $> 10^{12}$  Pa s (which corresponds to mixing times  $> 5 \times 10^5$  h). This is not a concern for  $\alpha$ -pinene SOA since the viscosity of  $\alpha$ -pinene SOA is rarely  $> 10^{12}$  Pa s in the PBL.

### S2. Calculations of vertical profiles of temperature and RH in the boundary layer above Hyytiälä (boreal forest) and the Amazon (rainforest)

33 The monthly average afternoon (13:00-15:00, local time) temperature and RH vertical profiles  
 34 over Hyytiälä and the Amazon were calculated for the driest month of the year at these locations.  
 35 For Hyytiälä, the average afternoon temperatures and RHs at the surface were obtained from the  
 36 SMEAR II campaign data set for 2012, retrieved from Etsin Research data finder  
 37 (<https://etsin.avointiede.fi/dataset>) (Aalto, 2012a, 2012b). For the Amazon, the temperature and  
 38 RH at the surface was obtained from NOAA's National Climate Data Center  
 39 (<http://www.ncdc.noaa.gov/>) from 2004 to 2014, and an average from five different stations was  
 40 used (Alfredo Vasquez Cobo, Itaituba, Tabatinga, Monte Dourado and Iauarete).

41 The temperature above the surface was calculated using a dry adiabatic lapse rate of 9.8 K km<sup>-1</sup>  
 42 and assuming that water vapour was well mixed within the PBL. To determine the RH at different  
 43 altitudes, the water vapor pressure, water saturated vapour pressure, and atmospheric pressure were  
 44 calculated. The atmospheric pressure was calculated using the following equation (Seinfeld and  
 45 Pandis, 2006):

$$46 \quad P(z) = P_0 \exp\left(-\frac{Mgz}{kT}\right) \quad (S3)$$

47 where P<sub>0</sub> is the standard pressure at sea level (101325 Pa), M is the molecular mass of the air (28.8  
 48 g/mol), g is the acceleration due to gravity (9.81 m s<sup>-2</sup>), z is the altitude in metres, k is the Boltzmann  
 49 constant and T is the temperature in Kelvin. The water saturated vapour pressure was calculated  
 50 using the Antoine equation (National Institute of Standards And Technology, 2016):

$$51 \quad \log_{10}(P) = A - \left(\frac{B}{T+C}\right) \quad (S4)$$

52 where P is the pressure, A=4.6543, B=1435.264, C=-64.848 and T is the temperature in Kelvin.  
 53 The values for A, B and C were based on the NIST values for water, which are valid for  
 54 temperatures between 256 and 373 K (National Institute of Standards And Technology, 2016).

55 In Fig. 5, the temperature and RH was plotted until the RH reached 100 %. The height at which  
 56 RH reached 100 % was only slightly lower than the average height of the planetary boundary layer  
 57 predicted by GEOS-5 meteorology data for the driest month of the year and for the afternoon  
 58 (13:00-15:00, local time) above Hyytiälä and the Amazon. For Hyytiälä, 100 % RH was reached  
 59 at 1605 m, while GEOS-5 predicted an average height of the PBL of 1667 m for this location and  
 60 time. For the Amazon, 100 % RH was reached at 882 m, while GEOS-5 predicted an average  
 61 height of the PBL of 1249 m for this location and time. When predicting the height of the PBL  
 62 using GEOS-5 meteorology, we ran GEOS-Chem at a horizontal grid resolution of 2° latitude by  
 63 2.5° longitude rather 4° latitude by 4.5° longitude to provide a better approximation to these single  
 64 locations. ö

### 65 **S3. Parametrization for the viscosity of sucrose particles as a function of temperature and** 66 **RH.**

67 We developed a parameterization for viscosity of sucrose particles as function of temperature and  
 68 RH by fitting the viscosity data listed in Table S5 to the following equation:

$$69 \quad \log(\eta) = 12 - \frac{C_1 * (T - \frac{w_{Suc} T_{gSuc} + w_{H2O} T_{gH2O} k_{GT}}{w_{Suc} + w_{H2O}})}{C_2 + (T - \frac{w_{Suc} T_{gSuc} + w_{H2O} T_{gH2O} k_{GT}}{w_{Suc} + w_{H2O}})} \quad (S5)$$

70 where  $C_1$  and  $C_2$  are constants,  $k_{GT}$  is the Gordon-Taylor fitting parameter,  $T_{gSuc}$  and  $T_{gH2O}$  are the  
 71 glass transition temperatures of dry sucrose and water and  $w_{Suc}$  and  $w_{H2O}$  are the weight fractions  
 72 of the dry sucrose and water in the particles. The weight fractions of dry sucrose and water in the  
 73 particles were determined from the RH using the following equation (Zobrist et al., 2011):

$$74 \quad \frac{RH}{100} = \frac{1 + aw_{Suc}}{1 + bw_{Suc} + cw_{Suc}^2} + (T - T^\theta)(dw_{Suc} + ew_{Suc}^2 + fw_{Suc}^3 + gw_{Suc}^4) \quad (S6)$$

75 where a-g are fitting parameters,  $T$  is the temperature in Kelvin and  $T^\theta$  is a reference temperature.  
 76 The values for  $T^\theta$  and a-g can be found in Table S6.

77 When fitting Eq. (S5) to the viscosity data for sucrose (Table S5), the parameters  $C_1$ ,  $C_2$ ,  $k_{GT}$  and  
 78  $T_{gSuc}$  were included as fitting parameters, while the glass transition temperature of water was fixed  
 79 at 135 K (Longinotti and Corti, 2008). The values for these parameters retrieved by fitting are  
 80 reported in Table S7. The  $T_{gSuc}$  value obtained by fitting was within the range measured  
 81 experimentally (319-335K) (Dette et al., 2014; Roos, 1993; Simperler et al., 2006).

82 Equation (S5) was based on the Williams, Landel and Ferry (WLF) equation and the Gordon-  
 83 Taylor equation, similar to Eq. (1) in the main text. Since the WLF equation is only valid at or  
 84 above the glass transition temperature, we have not used Eq. (S5) to predict viscosities above  $10^{12}$   
 85 Pa s (which corresponds to mixing times longer than  $5 \times 10^5$  h) (Fig. S2). If the temperature and  
 86 RH in the PBL was such that the viscosity was greater than  $10^{12}$  Pa s, we assigned a viscosity of  
 87  $10^{12}$  Pa s and a mixing time of  $5 \times 10^5$  hours. This assignment does not affect the conclusions in  
 88 this manuscript since a mixing time of  $5 \times 10^5$  hours is already well above the residence time of  
 89 SOA particles in the atmosphere. However, this assignment did lead to a relatively large frequency  
 90 count at  $5 \times 10^5$  hours in Fig. S4.

91

92

93

94 **References**

- 95 Aalto, P.: Hyytiälä SMEAR II meteorology, gases and soil- Relative humidity 16 m-2012, atm-  
96 data@helsinki.fi, Etsin Res. data finder [online] Available from:  
97 <https://etsin.avointiede.fi/dataset/urn-nbn-fi-csc-ida2014010802280s> (Accessed 28 June 2016a),  
98 2012.
- 99 Aalto, P.: Hyytiälä SMEAR II meteorology, gases and soil- Air temperature 8.4 m- 2012, atm-  
100 data@helsinki.fi, Etsin Res. data finder [online] Available from:  
101 <https://etsin.avointiede.fi/dataset/urn-nbn-fi-csc-ida2014010802682s> (Accessed 28 June 2016b),  
102 2012.
- 103 Bateman, A. P., Bertram, A. K. and Martin, S. T.: Hygroscopic Influence on the Semisolid-to-  
104 Liquid Transition of Secondary Organic Materials, *J. Phys. Chem. A*, 119(19), 4386–4395,  
105 doi:10.1021/jp508521c, 2015.
- 106 Crittenden, J. C., Trussel, R. R., Hand, D. W., Howe, K. J. and Tchobanoglous, G.: MWH's  
107 Water Treatment, John Wiley and Sons., 2012.
- 108 Dette, H. P., Qi, M. A., Schroder, D. C., Godt, A. and Koop, T.: Glass-Forming Properties of 3-  
109 Methylbutane-1,2,3-tricarboxylic Acid and Its Mixtures with Water and Pinonic Acid, *J. Phys.*  
110 *Chem. A*, 118(34), 7024–7033, doi:10.1021/jp505910w, 2014.
- 111 Först, P., Werner, F. and Delgado, A.: On the pressure dependence of the viscosity of aqueous  
112 sugar solutions, *Rheol. Acta*, 41(4), 369–374, doi:10.1007/s00397-002-0238-y, 2002.
- 113 Grayson, J. W., Zhang, Y., Mutzel, A., Renbaum-Wolff, L., Boege, O., Kamal, S., Herrmann, H.,  
114 Martin, S. T. and Bertram, A. K.: Effect of varying experimental conditions on the viscosity of  
115 alpha-pinene derived secondary organic material, *Atmos. Chem. Phys.*, 16(10), 6027–6040,  
116 doi:10.5194/acp-16-6027-2016, 2016.
- 117 Järvinen, E., Ignatius, K., Nichman, L., Kristensen, T. B., Fuchs, C., Hoyle, C. R., Höppel, N.,  
118 Corbin, J. C., Craven, J., Duplissy, J., Ehrhart, S., El Haddad, I., Frege, C., Gordon, H., Jokinen,  
119 T., Kallinger, P., Kirkby, J., Kiselev, A., Naumann, K. H., Petäjä, T., Pinterich, T., Prevot, A. S.  
120 H., Saathoff, H., Schiebel, T., Sengupta, K., Simon, M., Slowik, J. G., Tröstl, J., Virtanen, A.,  
121 Vochezer, P., Vogt, S., Wagner, A. C., Wagner, R., Williamson, C., Winkler, P. M., Yan, C.,  
122 Baltensperger, U., Donahue, N. M., Flagan, R. C., Gallagher, M., Hansel, A., Kulmala, M.,  
123 Stratmann, F., Worsnop, D. R., Möhler, O., Leisner, T. and Schnaiter, M.: Observation of  
124 viscosity transition in  $\alpha$ -pinene secondary organic aerosol, *Atmos. Chem. Phys.*, 16(7), 4423–  
125 4438, doi:10.5194/acp-16-4423-2016, 2016.
- 126 Longinotti, M. P. and Corti, H. R.: Viscosity of concentrated sucrose and trehalose aqueous  
127 solutions including the supercooled regime, *J. Phys. Chem. Ref. Data*, 37(3), 1503–1515,  
128 doi:10.1063/1.2932114, 2008.
- 129 Migliori, M., Gabriele, D., Di Sanzo, R., De Cindio, B. and Corraera, S.: Viscosity of  
130 multicomponent solutions of simple and complex sugars in water, *J. Chem. Eng. Data*, 52(4),  
131 1347–1353, doi:10.1021/je700062x, 2007.
- 132 National Institute of Standards And Technology: Water, [online] Available from:  
133 <http://webbook.nist.gov/cgi/cbook.cgi?ID=C7732185&Mask=4&Type=ANTOINE&Plot=on#ANTOINE>  
134 ANTOINE (Accessed 1 August 2016), 2016.
- 135 Perry, R. and Green, D.: Perry's Chemical Engineers' Handbook, McGraw-Hill, Toronto., 2008.

136 Power, R. M. and Reid, J. P.: Probing the micro-rheological properties of aerosol particles using  
 137 optical tweezers, *Reports Prog. Phys.*, 77(7), doi:10.1088/0034-4885/77/7/074601, 2014.  
 138 Quintas, M., Brandão, T. R. S., Silva, C. L. M. and Cunha, R. L.: Rheology of supersaturated  
 139 sucrose solutions, *J. Food Eng.*, 77(4), 844–852, doi:10.1016/j.jfoodeng.2005.08.011, 2006.  
 140 Roos, Y.: Melting and glass transitions weight carbohydrates of low molecular, *Carbohydr. Res.*,  
 141 238, 39–48, doi:10.1016/0008-6215(93)87004-C, 1993.  
 142 Seinfeld, J. H. and Pandis, S. N.: *Atmospheric Chemistry and Physics*, 2nd Ed., John Wiley and  
 143 Sons, Hoboken, NJ., 2006.  
 144 Simperler, A., Kornherr, A., Chopra, R., Bonnet, P. A., Jones, W., Motherwell, W. D. S. and  
 145 Zifferer, G.: Glass transition temperature of glucose, sucrose, and trehalose: An experimental and  
 146 in silico study, *J. Phys. Chem. B*, 110(39), 19678–19684, doi:10.1021/jp063134t, 2006.  
 147 Song, M. J., Liu, P. F. F., Hanna, S. J., Zaveri, R. A., Potter, K., You, Y., Martin, S. T. and  
 148 Bertram, A. K.: Relative humidity-dependent viscosity of secondary organic material from  
 149 toluene photo-oxidation and possible implications for organic particulate matter over megacities,  
 150 *Atmos. Chem. Phys.*, 16(14), 8817–8830, doi:10.5194/acp-16-8817-2016, 2016.  
 151 Swindells, J. F. and States., U.: Viscosities of sucrose solutions at various temperatures: tables of  
 152 recalculated values, , 7 [online] Available from: file://catalog.hathitrust.org/Record/007290919,  
 153 1958.  
 154 Telis, V. R. N., Telis-Romero, J., Mazzotti, H. B. and Gabas, a. L.: Viscosity of Aqueous  
 155 Carbohydrate Solutions at Different Temperatures and Concentrations, *Int. J. Food Prop.*, 10(1),  
 156 185–195, doi:10.1080/10942910600673636, 2007.  
 157 Zhang, Y., Sanchez, M. S., Douet, C., Wang, Y., Bateman, A. P., Gong, Z., Kuwata, M.,  
 158 Renbaum-Wolff, L., Sato, B. B., Liu, P. F., Bertram, A. K., Geiger, F. M. and Martin, S. T.:  
 159 Changing shapes and implied viscosities of suspended submicron particles, *Atmos. Chem. Phys.*,  
 160 15(14), 7819–7829, doi:10.5194/acp-15-7819-2015, 2015.  
 161 Zobrist, B., Marcolli, C., Pedernera, D. A. and Koop, T.: Do atmospheric aerosols form glasses?,  
 162 *Atmos. Chem. Phys.*, 8(17), 5221–5244, 2008.  
 163 Zobrist, B., Soonsin, V., Luo, B. P., Krieger, U. K., Marcolli, C., Peter, T. and Koop, T.: Ultra-  
 164 slow water diffusion in aqueous sucrose glasses, *Phys. Chem. Chem. Phys.*, 13(8), 3514–3526,  
 165 doi:10.1039/c0cp01273d, 2011.

166  
 167 **Tables**

168 **Table S1.** Room temperature  $\alpha$ -pinene SOA viscosity data used to create a parameterization for  
 169 the viscosity of  $\alpha$ -pinene SOA as a function of temperature and RH.

Reference	Viscosity (Pa s)	RH (%)	Temperature (K)
Grayson et al. (2016) (SOA generated with mass concentration =121 $\mu\text{g m}^{-3}$ )	<sup>a</sup> Range=1.8x10 <sup>2</sup> -1.5x10 <sup>4</sup> , midpoint=1.6 x10 <sup>3</sup>	50	<sup>c</sup> Range=293- 295 Midpoint=294
	<sup>a</sup> Range=9.8x10 <sup>2</sup> -3.0x10 <sup>4</sup> , midpoint=5.4 x10 <sup>3</sup>	40	
	<sup>a</sup> Range=4.6x10 <sup>3</sup> -1.4x10 <sup>5</sup> , midpoint=2.5x10 <sup>4</sup>	30	
	<sup>a</sup> Range=1.6x10 <sup>6</sup> -5.9x10 <sup>7</sup> , midpoint=9.6 x10 <sup>6</sup>	<sup>b</sup> 0	

Grayson et al. (2016) (SOA generated with a mass concentration = 520 $\mu\text{g m}^{-3}$ )	<sup>a</sup> Range=4.2x10 <sup>2</sup> -3.1x10 <sup>4</sup> , midpoint=3.6x10 <sup>3</sup>	50	
	<sup>a</sup> Range=9.7x10 <sup>2</sup> -7.9x10 <sup>4</sup> , midpoint=8.7x10 <sup>3</sup>	40	
	<sup>a</sup> Range=3.4x10 <sup>3</sup> -2.1x10 <sup>5</sup> , midpoint=2.6x10 <sup>4</sup>	30	
	<sup>a</sup> Range=3.5x10 <sup>5</sup> -1.8x10 <sup>7</sup> , midpoint=2.5x10 <sup>6</sup>	<sup>b</sup> 0	
Bateman et al. (2015)	1 x10 <sup>1</sup>	70	293
Zhang et al. (2015) <sup>d</sup>	2.3 x10 <sup>8</sup>	5.2	293
	1.3 x10 <sup>8</sup>	13.8	293
	3.2 x10 <sup>7</sup>	22.9	293
	1.4 x10 <sup>7</sup>	36.7	293
	6.0 x10 <sup>6</sup>	44.3	293
	5.1 x10 <sup>6</sup>	54.3	293

170 <sup>a</sup> Grayson et al. (2016) reported upper and lower limits to the viscosity (i.e. range) at each specified  
171 RH. To simplify the fitting procedure, we used the midpoints of the viscosities from Grayson et  
172 al (2016).

173 <sup>b</sup> Grayson et al. (2016) measured the viscosity under dry conditions (RH of < 0.5 % based on  
174 measurements). When developing the parameterization we used a value of 0 % RH.

175 <sup>c</sup> Grayson et al. (2016) carried out experiments at room temperature (293 K-295 K). We used the  
176 midpoint of the temperature (294 K) when developing the viscosity parameterization for  $\alpha$ -pinene  
177 SOA.

178 <sup>d</sup>Zhang et al. (2015) reported 36 measurements of viscosity over the range of 0 to 60%. For the  
179 fitting procedure, we binned their data by relative humidity and used the average viscosity and  
180 relative humidity in each bin. The width of each bin was approximately 10% RH. This binning  
181 procedure was carried out to give the data from Grayson et al. (2016) and Zhang et al. (2015)  
182 similar weights, since both were carried out at room temperature and over a similar RH range.

183 **Table S2.** Low temperature  $\alpha$ -pinene SOA viscosity data used to create a parameterization for the  
184 viscosity of  $\alpha$ -pinene SOA as a function of temperature and RH.

Reference	Viscosity (Pa s)	RH (%)	Temperature (K)
Järvinen et al. (2016)	1x10 <sup>7</sup>	<sup>a</sup> Range=22.9-36.3, midpoint=29.6	263.3
		<sup>a</sup> Range=30.5-37.3, midpoint=33.9	262.9
		<sup>a</sup> Range=40.5-46.0, midpoint=43.3	253.3
		<sup>a</sup> Range=44.0-49.8, midpoint=46.9	252.9
		<sup>a</sup> Range=55.0-63.4, midpoint=59.2	243.3
		<sup>a</sup> Range=68.6-80.1, midpoint=74.4	235.5

185 <sup>a</sup> Järvinen et al (2016) reported upper and lower limits to the RH for a specific temperature and  
 186 viscosity. To simplify fitting, we used the midpoint of the RH range.

187 **Table S3.** Liquid water viscosity data used to create a parameterization for the viscosity of  $\alpha$ -  
 188 pinene SOA as a function of temperature and RH.

Reference	Viscosity (Pa s)	RH (%)	Temperature (K)
Crittenden et al. (2012)	<sup>a</sup> 1.002x10 <sup>-3</sup>	100	293
	<sup>a</sup> 1.139 x10 <sup>-3</sup>		288
	<sup>a</sup> 1.307 x10 <sup>-3</sup>		283
	<sup>a</sup> 1.518 x10 <sup>-3</sup>		278
	<sup>a</sup> 1.781 x10 <sup>-3</sup>		273

189 <sup>a</sup> The viscosities values in Crittenden et al. (2012) were reported to 4 significant digits.

190 **Table S4.** Initial guess parameters and fitting parameters used in Eq. (1) to predict the viscosity of  
 191  $\alpha$ -pinene SOA as a function of temperature and RH. The fitting parameters were obtained by  
 192 fitting Eq. (1) to the viscosity data listed in Tables S1-S3.

Parameter	Guess Value	Fitting Value
C <sub>1</sub>	19	31297
C <sub>2</sub>	50 K	331446 K
K <sub>GT</sub>	2.5	5.155
T <sub>gSOA</sub>	250	245.17 K

193

194 **Table S5.** Literature viscosity data used to create a parameterization for the viscosity of sucrose  
 195 particles as a function of temperature and RH.

System	Viscosity Range (Pa s)	RH (%)	Temperature (K)	Reference
Water	1.002x10 <sup>-3</sup> to 1.781x10 <sup>-3</sup>	100	275-293	Crittenden et al. (2012)
Sucrose-water	3.19x10 <sup>-3</sup> to 4.82x10 <sup>-1</sup>	96.2-80	293	Swindells et al. (1958)
	6.73x10 <sup>-1</sup> to 1.10x10 <sup>3</sup>	80-56.6		Quintas et al. (2006)
	1.97x10 <sup>-3</sup> to 5.67x10 <sup>-2</sup>	99.4-88		Perry and Green (2008)
	1.25x10 <sup>-3</sup> to 8.30x10 <sup>-2</sup>	99.99-87.96		Migliori et al. (2007)
	1.26x10 <sup>-3</sup> to 7.65x10 <sup>-2</sup>	99.89-87.98		Telis et al. (2007)
	1.03x10 <sup>-3</sup> to 5.81x10 <sup>-2</sup>	100-87.98		Forst et al. (2002)

	$3 \times 10^{-2}$ to $6.71 \times 10^8$	92-28		Power and Reid (2014)
	$1 \times 10^{12}$	48.53-25.88	255-295 (5 degree increments) <sup>a</sup>	Zobrist et al. (2008)

196 <sup>a</sup> Zobrist et al. (2008) reported glass transition temperatures as a function of water activity for the  
197 range of 160 K to 300 K. These glass transition temperatures were based on glass transition  
198 temperature measurements in the range of 240 K to 180 K, water activity measurements, and the  
199 Gordon-Taylor equation. To develop our parameterization, we used their glass transition  
200 temperatures over the range of 255 K to 295 K from their Fig. 5b, recorded in 5 K increments.

201

202 **Table S6.** Parameters from Zobrist et al. (2011) used in Eq. (S6) to predict the weight fractions of  
203 sucrose and water in particles as a function of relative humidity.

Parameter	Value	Parameter	Value
a	-1	e	-0.005151
b	-0.99721	f	0.009607
c	0.13599	g	-0.006142
d	0.001688	T <sup>o</sup>	298 K

204

205 **Table S7.** Fitting parameters used in Eq. (S5) to predict the viscosity of sucrose particles as a  
206 function of temperature and RH. These parameters were obtained by fitting Eq. (S5) to the  
207 viscosity data listed in Table S5 as well as the guess values in the table.

Parameter	Guess Value	Fitting Value
C <sub>1</sub>	19	20.06
C <sub>2</sub>	50 K	55.58 K
K <sub>GT</sub>	4.74	4.531
T <sub>gSOA</sub>	336 K	324.5 K

208

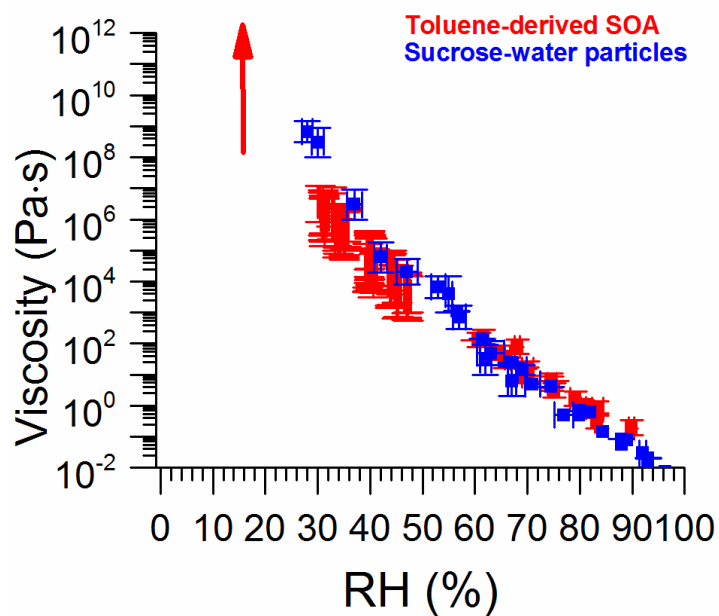
209



210

211 **Figures**

212



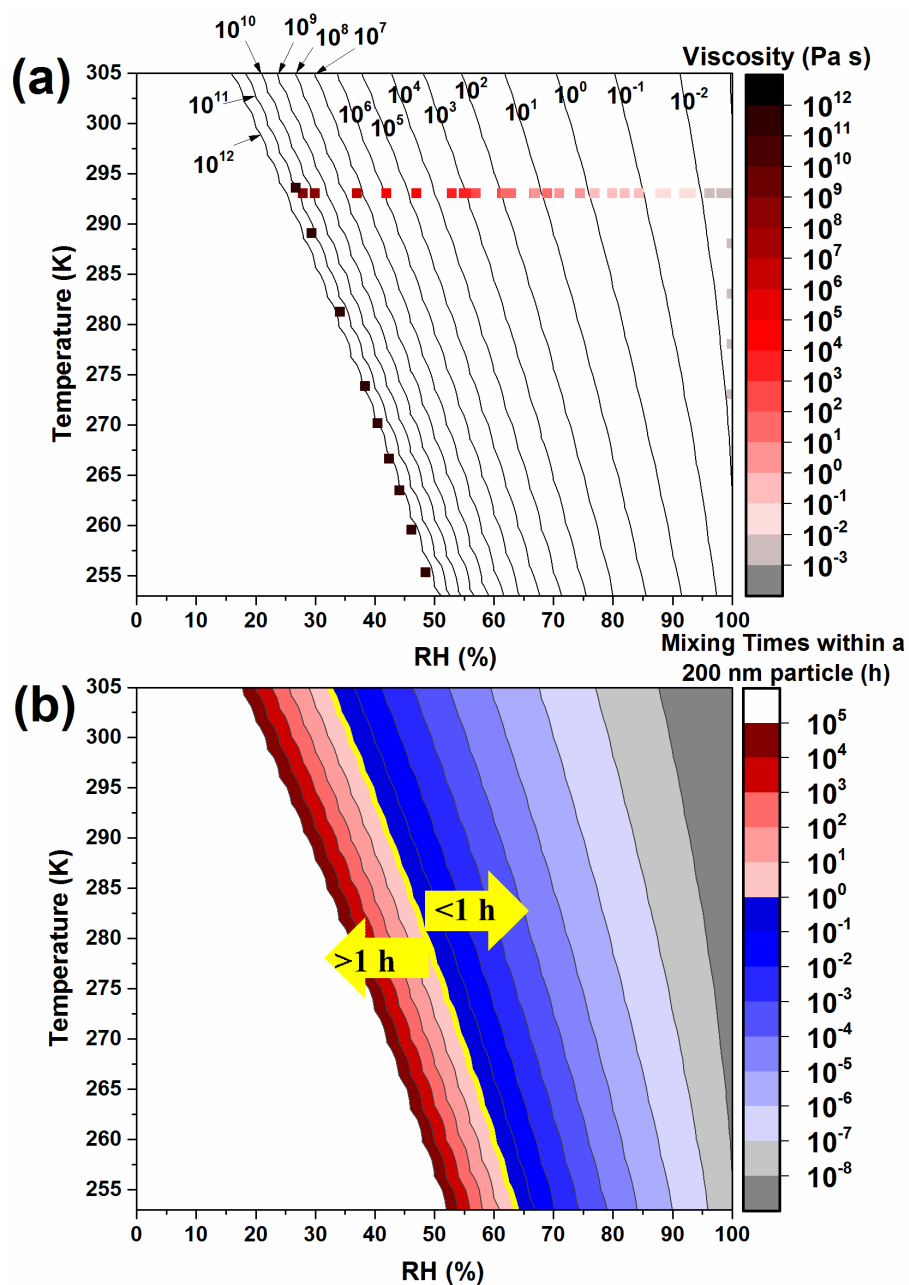
213

214 **Figure S1.** Viscosities of different proxies of anthropogenic SOA as a function of RH. Data for  
215 toluene SOA taken from Song et al. (2016). The data for sucrose-water mixtures was taken from  
216 Swindells (1958), Quintas et al. (2006), Telis et al. (2007), Forst et al. (2002), Migliori et al. (2007),  
217 Perry and Green (2008), and Power and Reid (2014).

218

219

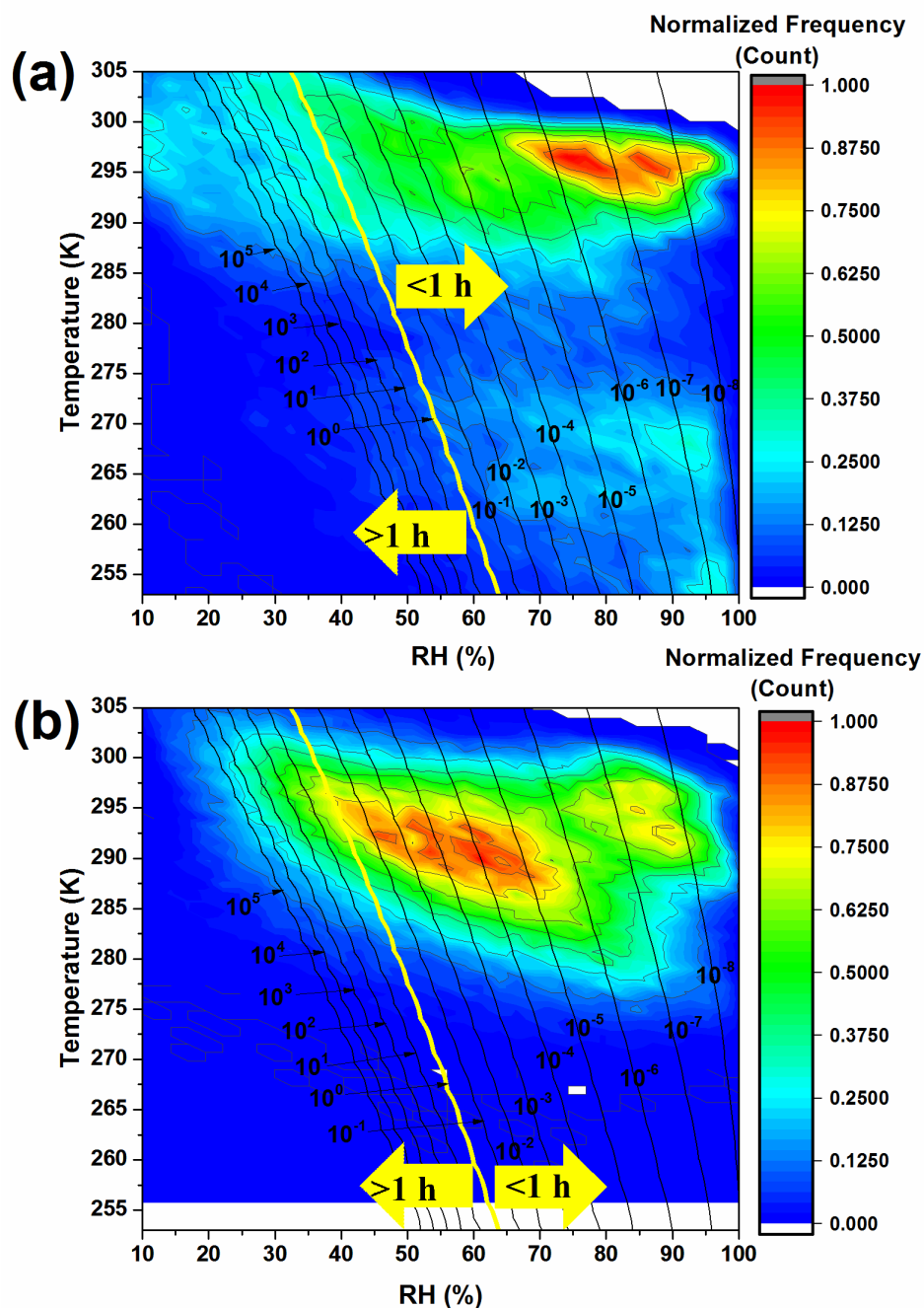
220



221

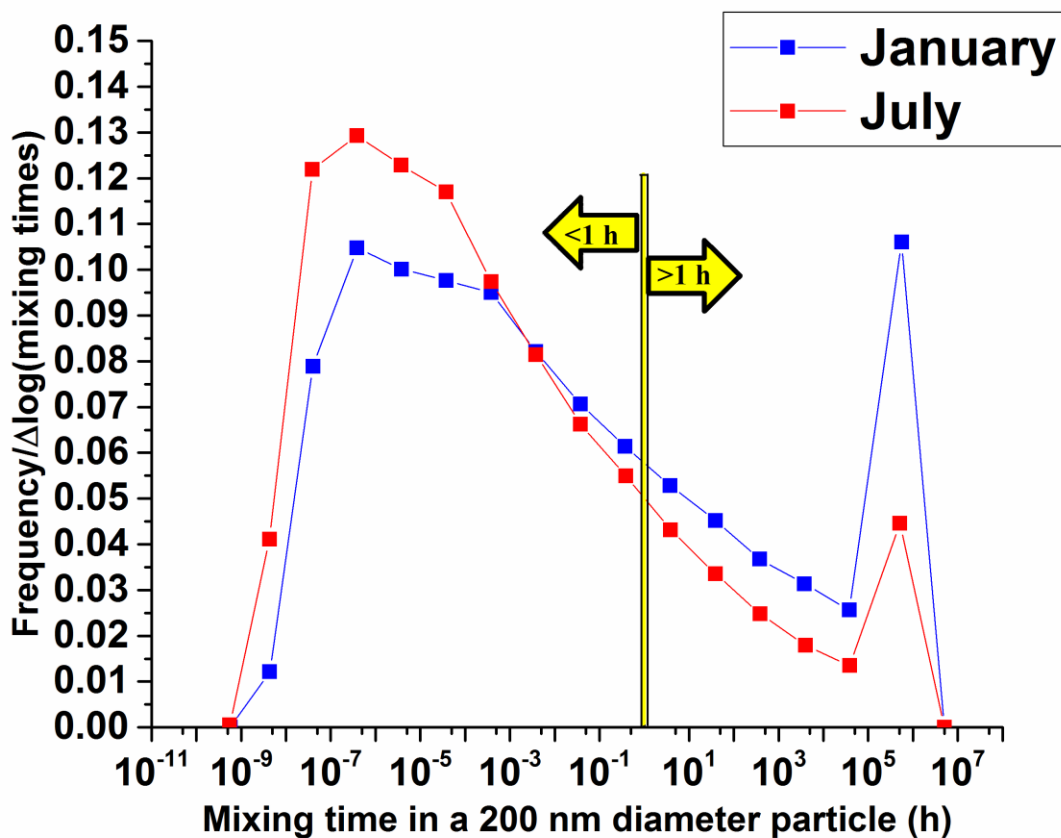
222 **Figure S2.** Panel A: Parameterization (contours) for the viscosity of sucrose particles (as  
 223 surrogates of toluene SOA) as a function of temperature and RH and measured viscosities used to  
 224 construct the parameterization (symbols). The measured viscosities are listed in Table S5. Panel  
 225 B: Mixing times (color scale) for organic molecules within 200 nm sucrose particles as a function  
 226 of temperature and RH. Mixing times were calculated from the viscosity parameterization (Panel  
 227 A) and Eq. (3) and (4) in the main text.

228



229

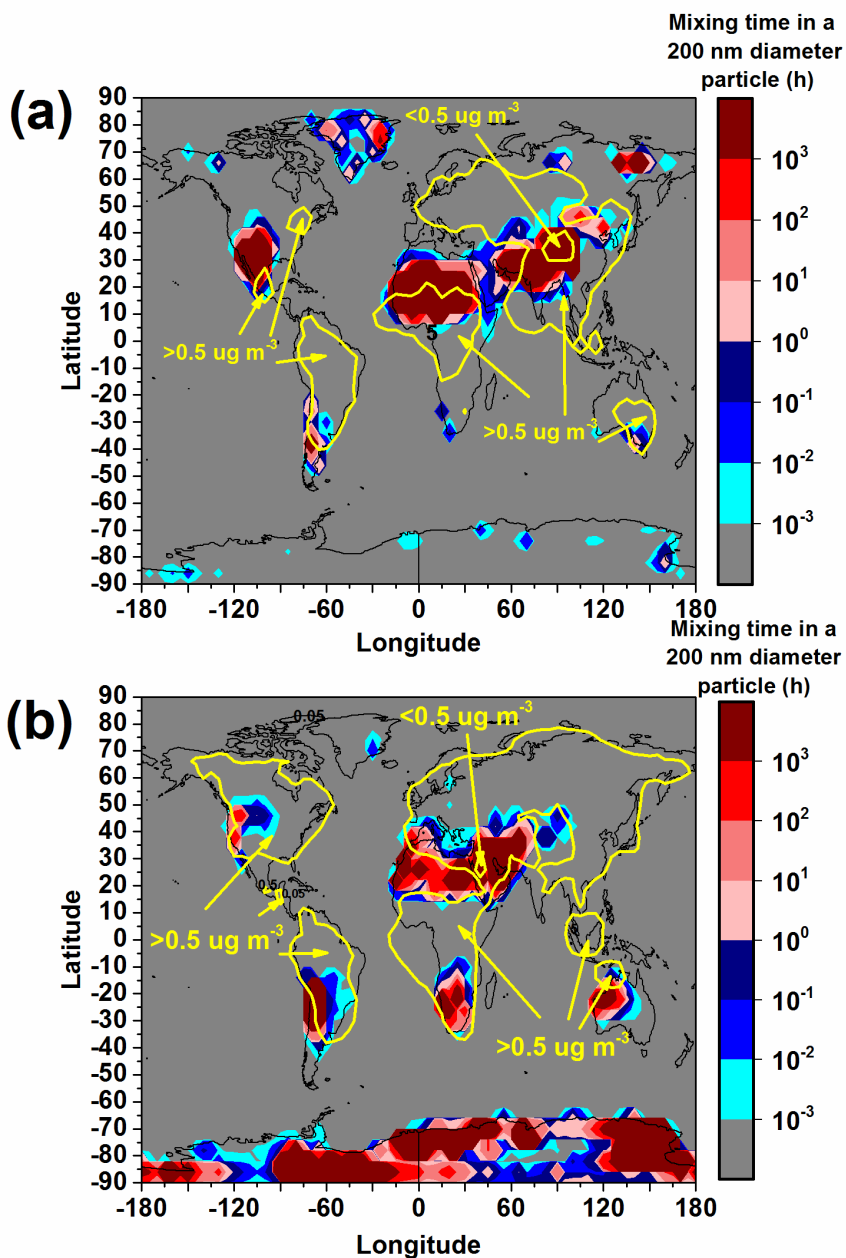
230 **Figure S3.** Six-hour normalized frequency counts of temperature and RH in the planetary  
 231 boundary layer (color scale) together with the mixing times for organic molecules within 200 nm  
 232 sucrose particles (as surrogates of toluene SOA) (contours). Panel A and B show the conditions  
 233 for January and July, respectively. Mixing times (contours) are reported in hours. Frequency  
 234 counts in the PBL were only included for the conditions when the mass concentration of total  
 235 organic aerosol was  $> 0.5 \mu\text{g}/\text{m}^3$  at the surface.



237

238 **Figure S4.** Normalized frequency distributions of mixing times within sucrose particles (as  
 239 surrogates for toluene SOA) in the planetary boundary layer. Red symbols corresponds to January  
 240 and blue symbols corresponds to July. Frequency counts in the PBL were only included for the  
 241 conditions where the mass concentration of total organic aerosol was  $> 0.5 \mu\text{g m}^{-3}$  at the surface.  
 242 The relatively large frequency count at  $5 \times 10^5$  h is because all cases that had a viscosity greater  
 243 than  $10^{12}$  Pa s, it was assigned a value of  $10^{12}$  Pa s. For additional details see Section S3.

244



245

246 **Figure S5.** Mixing times of organic molecules within 200 nm sucrose particles (as surrogates of  
 247 toluene SOA) at the top of the planetary boundary layer as a function of latitude and longitude.  
 248 The color scale represents mixing times and the yellow contours illustrate when the concentration  
 249 of total organic aerosol is  $> 0.5 \mu\text{g m}^{-3}$  at the surface. Panel A and B correspond to January and  
 250 July, respectively.

251